International Journal of Modelling and Simulation

ISSN: 0228-6203 (Print) 1925-7082 (Online) Journal homepage: www.tandfonline.com/journals/tjms20

Modelling and Simulation of Direct Torque Controlled Induction Motor Drive using Slip Speed Control

Vinay T. Kumar & Srinivasa S. Rao

To cite this article: Vinay T. Kumar & Srinivasa S. Rao (2013) Modelling and Simulation of Direct Torque Controlled Induction Motor Drive using Slip Speed Control, International Journal of Modelling and Simulation, 33:2, 109-116, DOI: 10.2316/Journal.205.2013.2.205-5766

To link to this article: https://doi.org/10.2316/Journal.205.2013.2.205-5766

Published online: 15 Jul 2015.

MODELLING AND SIMULATION OF DIRECT TORQUE CONTROLLED INDUCTION MOTOR DRIVE USING SLIP SPEED CONTROL

Vinay T. Kumar* and Srinivasa S. Rao*

Abstract

In this paper an effective control strategy to reduce the torque and flux ripple in direct torque control (DTC) of induction motor drive based on a slip speed control of stator flux is presented. This control strategy is applied to three-level inverter configuration using cascaded two two-level inverters for improving the performance of the system. Torque control is achieved by reference stator flux angle which is generated from the sum of incremental change in stator flux angle and actual stator flux angle. Modelling and simulation of proposed DTC is presented and results of the simulation are compared with basic DTC. From the simulation results it is observed that the torque and flux ripple are less with proposed DTC and also an improvement in the steady-state performance of the drive system at high and low speed operation.

Key Words

Direct torque control, direct flux control, induction motor, space vector modulation, three-level inverter

1. Introduction

In order to eliminate the drawbacks of field orientation control (FOC) of induction motor drives [1], in 1985 Takahashi and Noguchi proposed a technique is called direct torque control (DTC) method [2]. In DTC coordinate transformations are replaced by bang-bang controllers *i.e.*, hysteresis controllers. The operation of the DTC is based upon application of a suitable voltage vector for a given sample time to keep flux and torque errors within a specified hysteresis band and provide independent control of flux and torque. Inverter switching frequency of conventional DTC is not constant and only one voltage space vector is applied for the entire sampling period and also it produces high ripple in torque and flux due to non-linear hysteresis controllers [3]–[5]. To overcome this problem, a torque ripple minimization algorithm was proposed based on calculation of duty cycle with constant switching frequency operation [6] but at the expense of mathematical complexity. To achieve the constant switching frequency and reduce torque ripple, space vector modulation (SVM)-DTC control technique was proposed in [7], which is based on stator flux coordination technique [8]–[10]. But, it is parameter sensitivity and decreases the system performance in flux weakening conditions. In [11], another technique was proposed to improve the low-speed performance of the DTC by eliminating the null voltage vector from the voltage switching table of basic DTC but still switching frequency is uncontrolled. Some researchers have proposed a dithering technique for DTC to improve system performance and also increase the inverter switching frequency by injecting small amplitude of high-frequency triangle signal to flux and torque errors [12], but it requires high sampling frequency than SVM-DTC technique. In [13], proposed a scheme to reduce flux and torque ripple and also achieved constant inverter switching frequency operation. But it requires high sampling frequency triangle signals. In [14], proposed a scheme to introduce more zero and/or non-zero voltage vectors to the basic switching table which results in the reduction of torque and flux ripple without need of modulation technique. But performance is poor under low-speed operation. Later researchers proposed different techniques for improving the basic DTC performance were reported in [15]. The DTC algorithm has been extended from low-power ratings into medium-power motor drives application area. The advantages of the three-level inverters are high voltage, high power with fewer harmonic in the output with optimum switching frequency was reported in [16]. Most of the three-level inverter DTC methods are based on clamping inverters [17], [18]. But they suffer with fluctuating neutral point due to DC link capacitor currents. By using H-Bridge topology, these problems can be eliminated. But they require more than two isolated power supplies. To eliminate the neutral point fluctuations, cascading topology of two two-level inverter was proposed in

* Department of Electrical Engineering, National Institute of Technology, Warangal, A.P., 506007, India; e-mail: tvinay.nitw@gmail.com; srinivasarao_nitw@yahoo.co.in

Recommended by Dr. M.H. Hamza
(DOI: 10.2316/Journal.205.2013.2.205-5766)

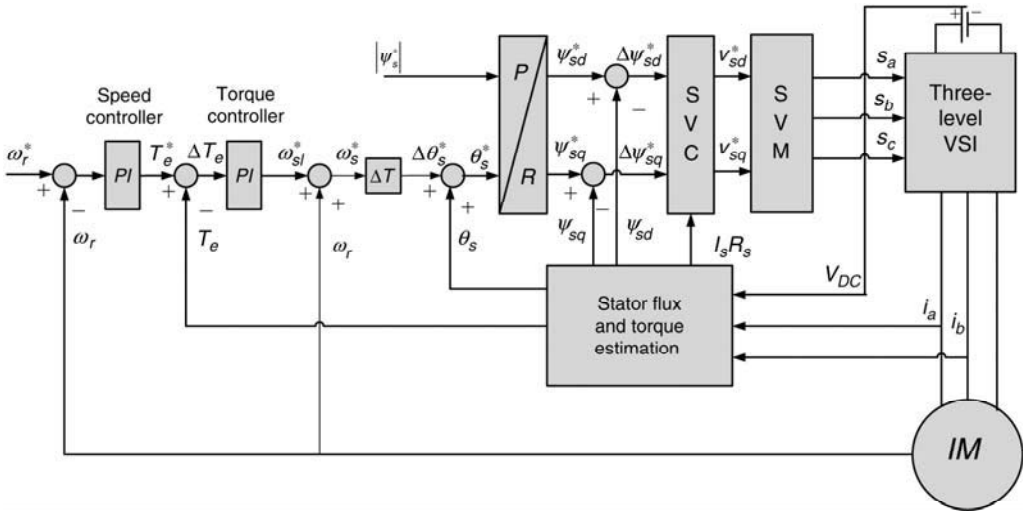

Figure 1. Proposed DTC method using cascaded two two-level inverters.

[19]. In [18], a new technique was applied to three-level inverter to DTC for reduce the torque and flux ripple based on current ripple principle, but switching frequency is uncontrolled and torque and flux ripple are high at low-speed operation. This paper advances the authors previous work [20], in which problems associated with basic DTC were outlined and a solution was proposed by applying a suitable control scheme to two-level inverter. This paper deals with a new control logic to DTC for cascaded two two-level inverters in which the inverter switching frequency is maintained constant, as a result flux and torque ripple in high- and low-speed operation are reduced by slip speed control of stator flux.

2. Proposed DTC Method using Cascaded Two Two-Level Inverters

The proposed DTC of induction motor with three-level inverter configuration using cascaded two two-level inverters as shown in Fig. 1. In this scheme, voltage switching table and hysteresis controllers are eliminated. Prediction of the reference stator flux unit, polar (P) to rectangular (R) transformation unit, the reference stator voltage calculation (SVC) unit, and SVM units are added. In this control strategy, torque control is achieved by slip speed control of stator flux. From (1), it is clear that electromagnetic torque T_e control is directly performed by changing the load angle δ with maintaining stator flux ψ_s and rotor flux ψ_r magnitudes are constant. Using [21], (1) can be derived as (2).

$$T_e = (3p/2)|\psi_s||\psi_r'|\sin\delta \tag{1}$$

$$T_e(t) = \left[\frac{3}{2}p\frac{L_m^2}{R_rL_s^2}|\psi_s^2|\right]\left[1-e^{-t/\tau}\right](\omega_s-\omega_r) \tag{2}$$

where $\tau = \sigma L_r/R_r$ is the rotor time constant, σ is the leakage coefficient, R_r is the rotor resistance, p is the number of pole pare, L_s, L_r, and L_m are the stator, rotor, and mutual inductances, respectively. From (2), $(\omega_s-\omega_r)$ is called slip speed ω_{slip} of the stator flux angular speed ω_s and rotor angular speed ω_r in rad/s. The slip angular frequency ω_{slip} can be written as:

$$\omega_{slip} = \omega_s - \omega_r \tag{3}$$

By substituting, (3) in (2), the instantaneous electromagnetic torque T_e is:

$$T_e(t) = \left[\frac{3}{2}p\frac{L_m^2}{R_rL_s^2}|\psi_s^2|\right]\left[1-e^{-t/\tau}\right](\omega_{slip}) \tag{4}$$

From (4), the electromagnetic torque is directly controlled by slip angular speed ω_{slip}. The slip angular speed ω_{slip} can be rewritten as:

$$\omega_{slip} = \frac{d\theta_{slip}}{dt} = \frac{\Delta\theta_{slip}}{\Delta t} \tag{5}$$

From (5), $\Delta\theta_{slip}$ is the slip angle and Δt is the sampling time. Substituting (5) into (4), the modified instantaneous electromagnetic torque T_e is given by:

$$T_e(t) = \left[\frac{3}{2}p\frac{L_m^2}{R_rL_s^2}|\psi_s^2|\right]\left[1-e^{-t/\tau}\right]\left(\frac{\Delta\theta_{slip}}{\Delta t}\right) \tag{6}$$

From (6), it is clear that the electromagnetic torque T_e is directly controlled using slip angle per given sample time Δt. From [2], stator voltage equation is written by (7):

$$d\psi_s/dt = v_s - i_sR_s \tag{7}$$

where ψ_s is the stator flux, v_s is the voltage space vector, i_sR_s is the stator winding resistive voltage drop and Δt is the sample time. By neglecting stator winding resistive voltage drop, (7) becomes:

$$\Delta\psi_s = v_s\Delta t \tag{8}$$

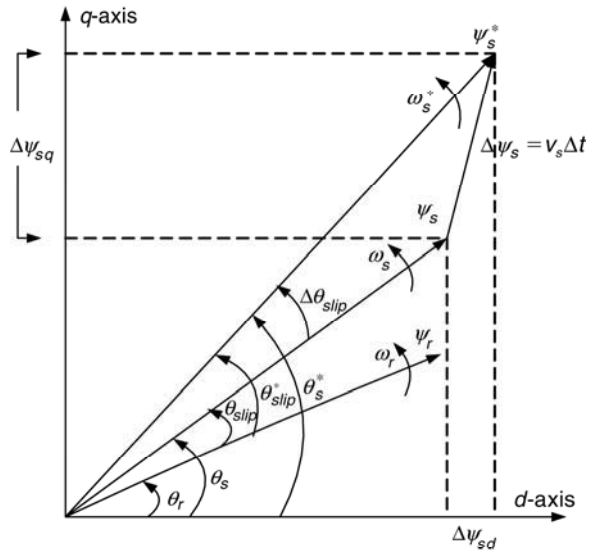

Figure 2. Compensation of stator flux error and torque error using stator flux control.

From (6) and (8), it is clear that the torque error and flux error are compensated by using voltage space vector v_s. Fig. 2 describes about how the stator flux error and torque error are compensated by voltage space vector v_s in a given sample time Δt based on direct flux control method.

From Fig. 1, the torque error ΔT_e and flux error $\Delta\psi_s$ will be compensated by applying suitable voltage vector v_s for particular sample time Δt, results the actual stator flux angle changed from θ_s to $\theta_s + \Delta\theta_{slip}$ without disturbing the flux magnitude and the actual stator flux magnitude chanced from ψ_s to ψ_s^* without disturbing the flux angle. From Fig. 2, the reference stator flux vector ψ_s^* is resolved in to d-axis reference flux ψ_{sd}^* and q-axis reference flux ψ_{sq}^* using reference flux angle θ_s^* given by (9).

$$\psi_{sd}^* + j\psi_{sq}^* = \psi_s^* \cos(\theta_s^*) + j\psi_s^* \sin(\theta_s^*) \tag{9}$$

The stator flux error $\Delta\psi_s$ is given by:

$$\Delta\psi_s = \psi_s^* - \psi_s \tag{10}$$

The reference voltage space vector v_s^* is given by:

$$v_s^* = \Delta\psi_s/\Delta t + i_s R_s \tag{11}$$

where $i_s R_s$ is stator resistive voltage drop. The reference stator flux vectors are designed from (9). $\Delta\psi_s$ is the stator flux error between reference stator flux and estimated actual stator flux. To reduce this stator flux error, required reference voltage space vector components are calculated from (11). Using this reference voltage space vector components, the time signals are calculated as explained in [22]. These time signals generate the controlled pulses for the voltage source inverter (VSI).

The three-level inverter configuration using cascaded two two-level inverters are shown in Fig. 3 and inverter

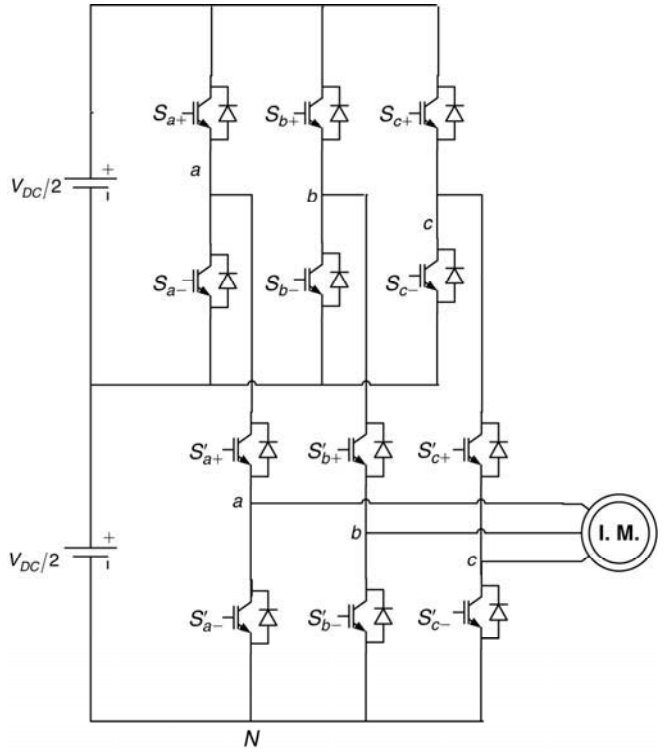

Figure 3. Three-level inverter using cascading of two two-level inverters [19].

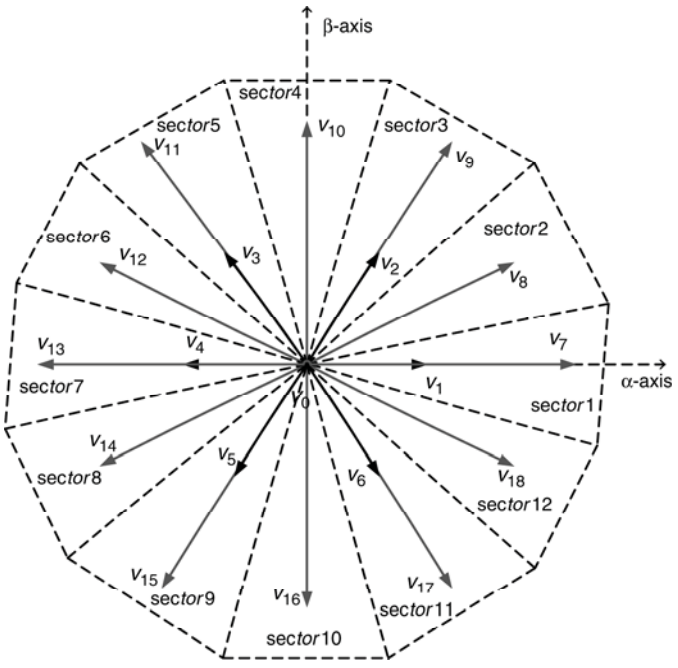

Figure 4. Space voltage vectors in three-level inverter.

voltage switching states are shown in Fig. 4. The voltage space vectors from v_1 to v_6 be useful for low-speed operating frequency and from v_7 to v_{18} be useful for high-speed operating frequency conditions.

The switching states for phase "a" are represented in Table 1.

Table 1
Switching States of Phase "a" Leg

	S_{a+}	S'_{a+}	S_{a-}	S'_{a-}	Pole Voltage V_{aN}
Switching Status of Phase A- Leg	ON	ON	OFF	OFF	V_{dc}
	OFF	ON	ON	OFF	$V_{dc}/2$
	OFF	OFF	OFF	ON	0

3. Simulation Results

From the developed mathematical models of the two- and three-level inverters, three-phase induction motor and control logic simulations were carried based on MATLAB/SIMULINK. Figure 5 shows the simulation results of basic DTC for forward motoring operation of induction motor drive speed at 1000 rpm (high speed), corresponding developed torque and stator flux. Figures 6 and 7 show the developed torque and stator flux of two- and three-levels proposed DTC at 1000 rpm, respectively. Figures 8–10 show torque ripple comparison of basic DTC and proposed DTC at 1000 rpm. Figures 11–13 show the comparison of stator flux ripple for basic DTC and proposed DTC at 1000 rpm.

From Figs. 14–16 represent the stator three-phases current and from Figs. 17–19 represent the d-axis phase voltage at 1000 rpm for basic DTC and proposed two- and three-levels DTC. Figures 20–25 show the torque ripple comparison and stator flux ripple of basic DTC and proposed DTC at 100 rpm (low speed). From Figs. 6 and 7, it is observed that the torque dynamic response is similar to basic DTC but steady-state flux and torque ripple are decreased compared with Fig. 5. From Figs. 8–10, it is

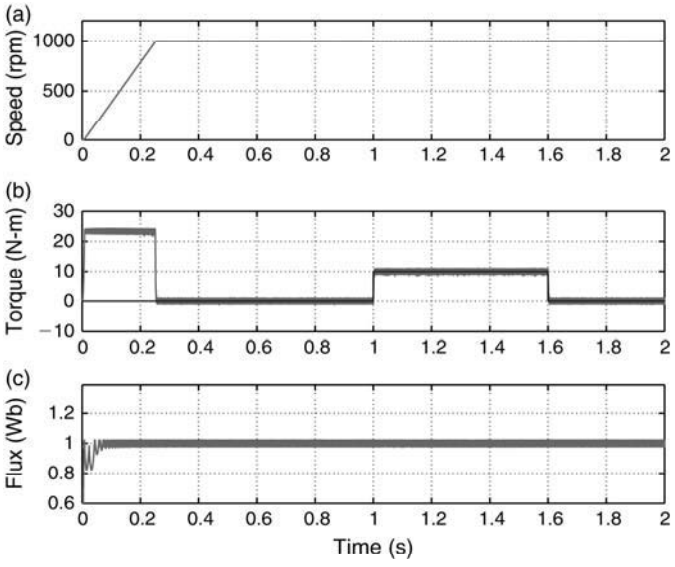

Figure 5. Simulation results of basic DTC: (a) variation of rotor speed from 0 to 1000 rpm; (b) load torque of 10 N-m is applied at 1 s and removed at 1.6 s; (c) stator flux.

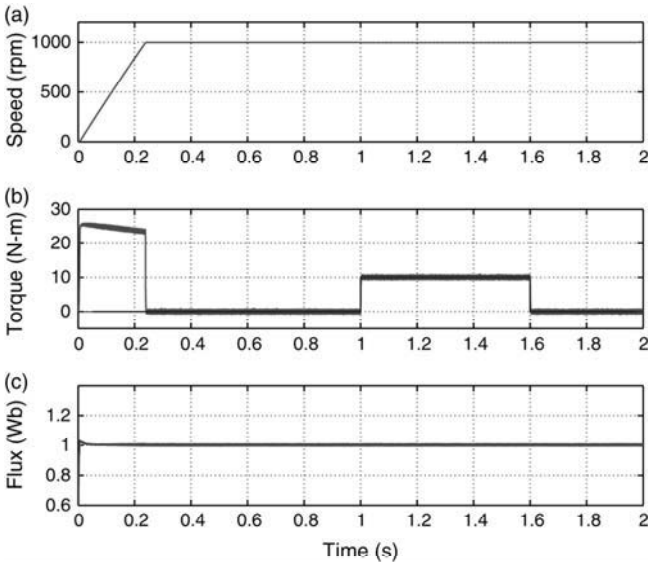

Figure 6. Simulation results of proposed two-level DTC: (a) variation of rotor speed from 0 to 1000 rpm; (b) load torque of 10 N-m is applied at 1 s and removed at 1.6 s; (c) stator flux.

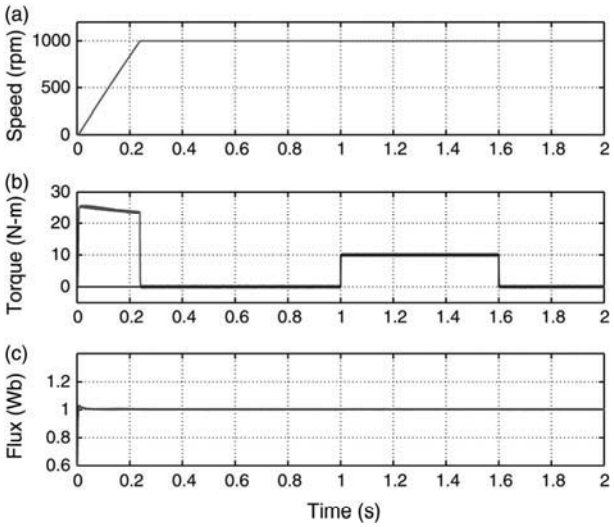

Figure 7. Simulation results of proposed three-level DTC: (a) variation of rotor speed from 0 to 1000 rpm; (b) load torque of 10 N-m is applied at 1 s and removed at 1.6 s; (c) stator flux.

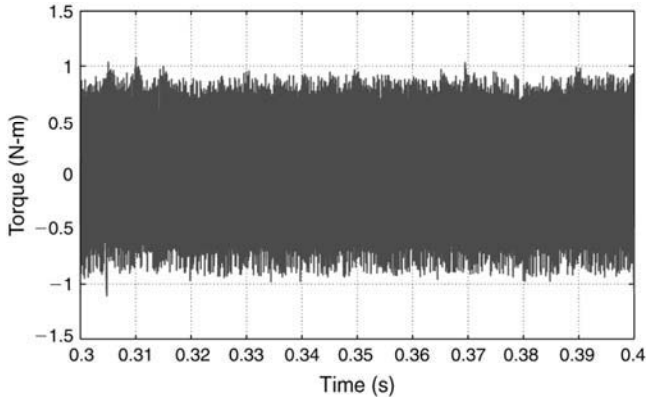

Figure 8. Simulation results of basic DTC: steady-state torque ripple at 1000 rpm speed.

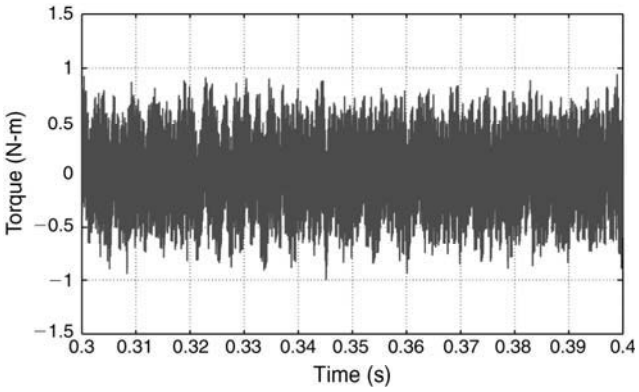

Figure 9. Simulation results of two-level DTC: steady-state torque ripple at 1000 rpm speed.

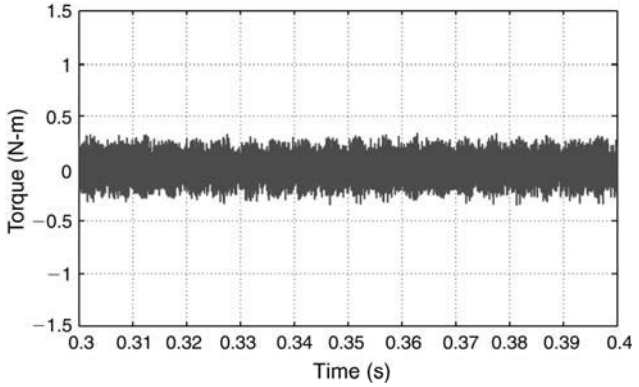

Figure 10. Simulation results of three-level DTC: steady-state torque ripple at 1000 rpm speed.

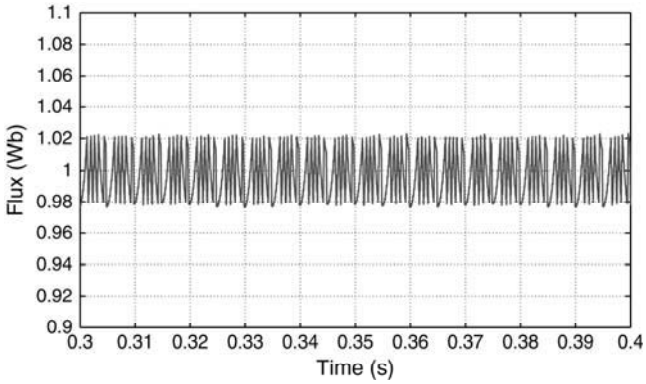

Figure 11. Simulation results of basic DTC: steady-state flux ripple at 1000 rpm speed.

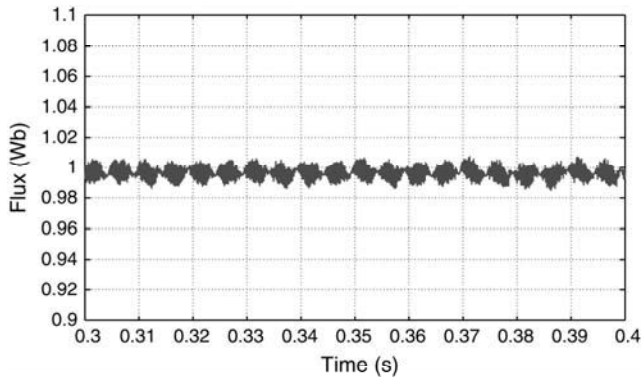

Figure 12. Simulation results of two-level DTC: steady-state flux ripple at 1000 rpm speed.

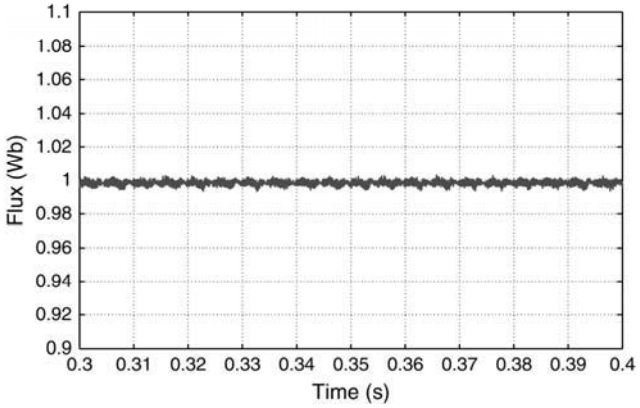

Figure 13. Simulation results of three-level DTC: steady-state flux ripple at 1000 rpm speed.

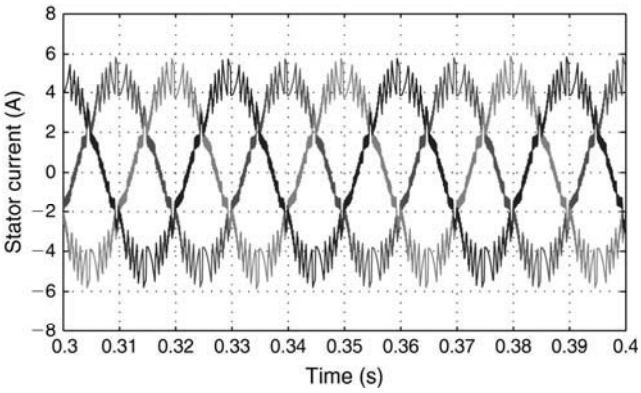

Figure 14. Simulation results of basic DTC: steady-state stator current at 1000 rpm speed.

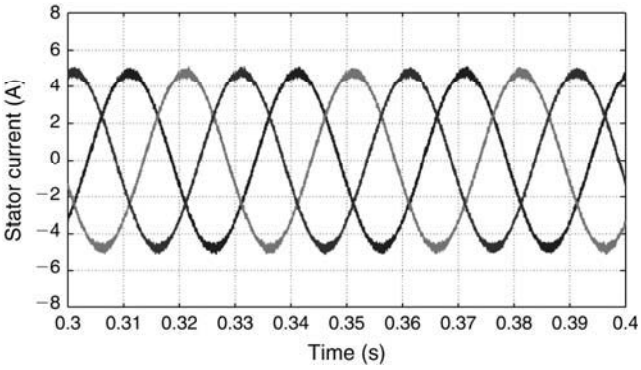

Figure 15. Simulation results of proposed two-level DTC: steady-state stator current at 1000 rpm speed.

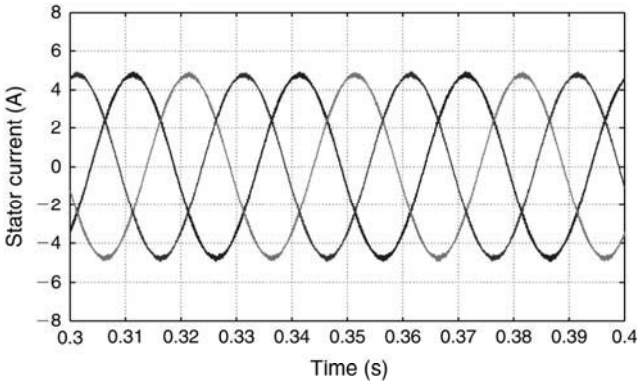

Figure 16. Simulation results of proposed three-level DTC: steady-state stator current at 1000 rpm speed.

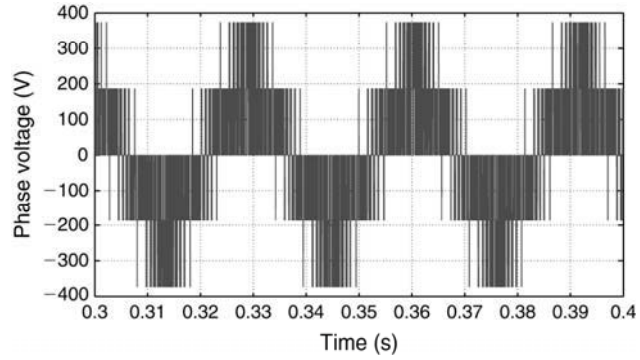

Figure 17. Simulation results of basic DTC: phase voltage at 1000 rpm.

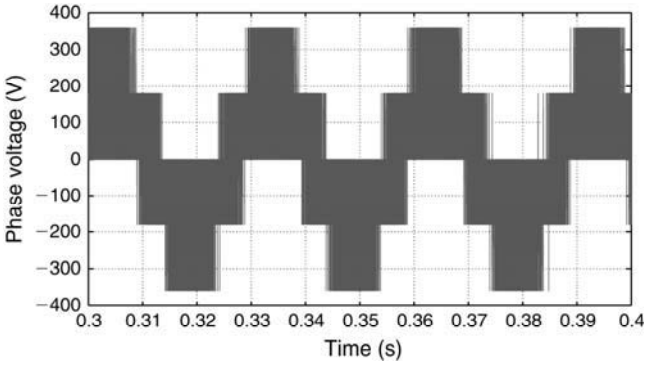

Figure 18. Simulation results of proposed two-level DTC: phase voltage at 1000 rpm.

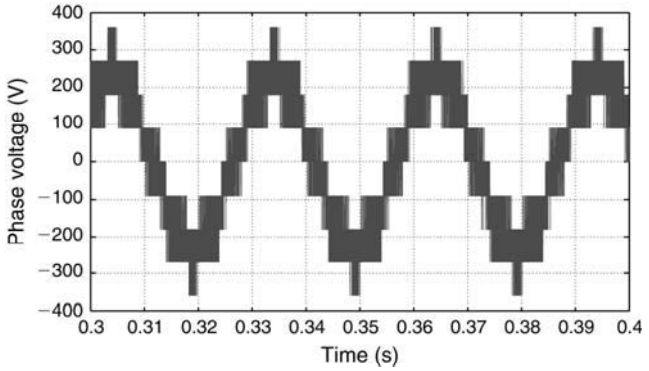

Figure 19. Simulation results of proposed three-level DTC: phase voltage at 1000 rpm.

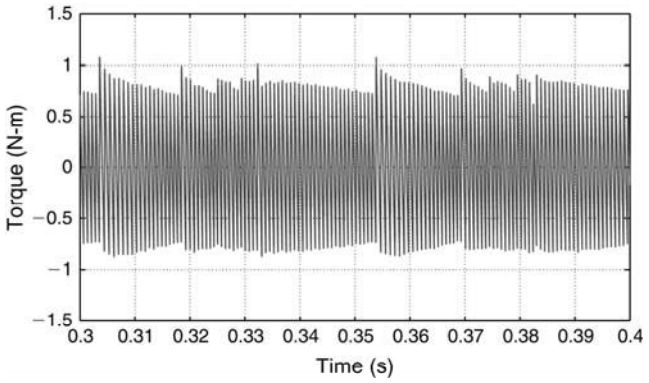

Figure 20. Simulation results of basic DTC: steady-state torque ripple at 100 rpm.

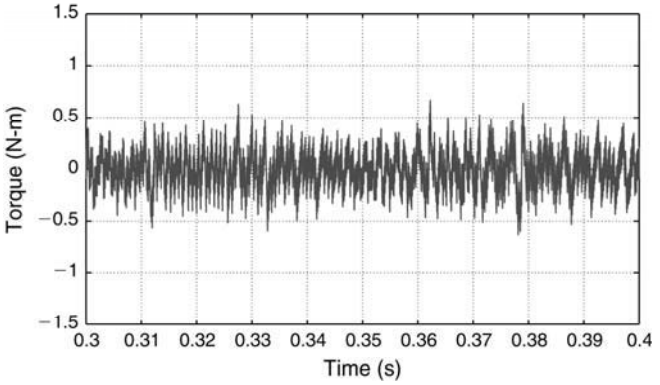

Figure 21. Simulation results of two-level proposed DTC: steady-state torque ripple at 100 rpm.

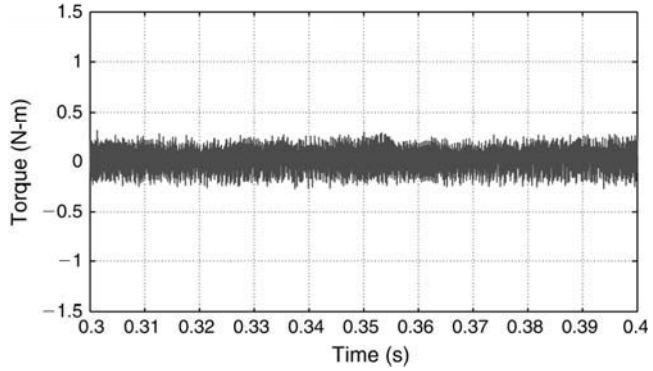

Figure 22. Simulation results of three-level proposed DTC: steady-state torque ripple at 100 rpm.

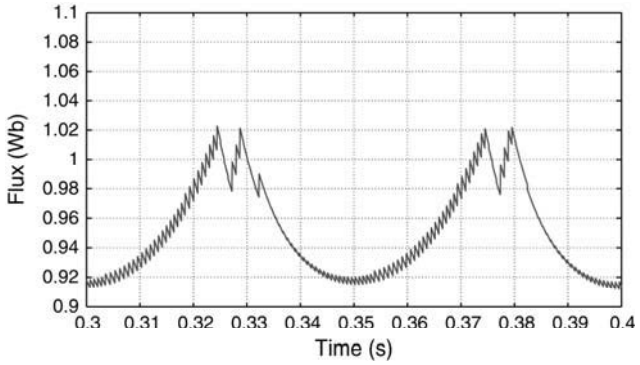

Figure 23. Simulation results of basic DTC: steady-state flux ripple at 100 rpm.

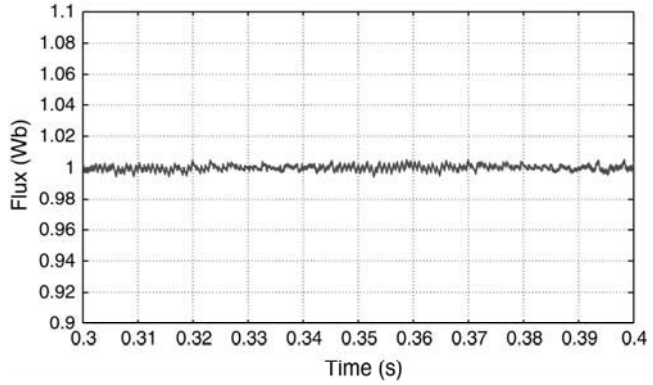

Figure 24. Simulation results of two-level proposed DTC: steady-state flux ripple at 100 rpm.

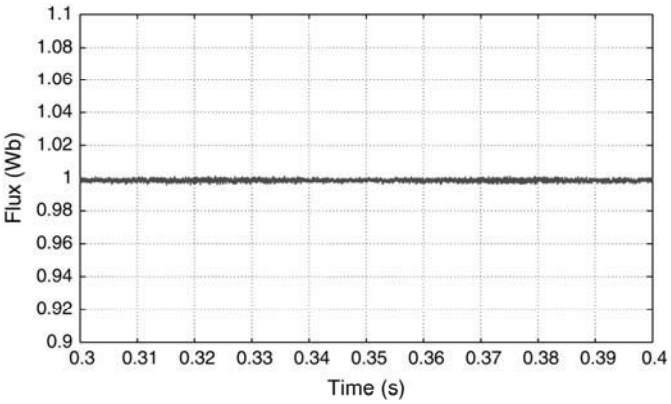

Figure 25. Simulation results of three-level proposed DTC: steady-state flux ripple at 100 rpm.

observed that torque ripple is less in three-level proposed DTC compared with basic DTC and two-level proposed DTC. From Figs. 11–13, it is observed that flux ripple is less in three-level proposed DTC compared with basic DTC and two-level proposed DTC. Figures 20–22 show torque ripple comparison of basic DTC and proposed DTC at 100 rpm (low speed). It is observed that torque ripple is decreased in three-level proposed DTC, when compared with basic DTC and two-level proposed DTC. Figures 23–25 show a stator flux ripple comparison of basic DTC and proposed DTC at 100 rpm motor speed. It is observed that flux ripple is decreased in three-level proposed DTC, when compared with basic DTC and two-level proposed DTC. From the above observations it is found that at 1000 and 100 rpm the torque and flux ripple are reduced using proposed scheme, when compared with basic DTC and two-level DTC methods.

4. Conclusion

In this paper, an algorithm for direct torque and flux control to reduce flux and torque ripple in a three-phase induction motor drive fed from a three-level inverter configuration consists of two cascaded two-level inverters was proposed. The torque control is achieved by reference stator flux angle which was generated from the sum of incremental change in stator flux angle and actual stator flux angle. The behaviour of the drive at high- and low-speed operation was observed. In both cases the torque and flux ripples are less when compared with basic DTC. The performance of the drive at low speed is better in particular.

References

[1] F. Blaschke, The principle of field-orientation as applied to the transvector closed-loop control system for rotating-field machines, *Siemens Review*, *34*, 1972, 217–220.

[2] I. Takahashi and T. Noguchi, A new quick-response and high-efficiency control of an induction motor, *IEEE Transactions on Industry Applications*, *22*(5), 1986, 820–827.

[3] D. Casadei, F. Profumo, G. Serra, and A. Tani, FOC and DTC: Two viable schemes for induction motors torque control, *IEEE Transactions on Power Electronics*, *17*, 2002, 779–787.

[4] D. Telford, M.W. Dunnigan, and B.W. Williams, A comparison of vector control and direct torque control of an induction machine, *Proc. IEEE PESC'00*, 2000, Galway, Ireland, 421–426.

[5] J.N. Nash, Direct torque control, induction motor vector control without an encoder, *IEEE Transactions on Industry Applications*, *33*, 1997, 333–341.

[6] J.-K. Kang and S.-K. Sul, New direct torque control of induction motor for minimum torque ripple and constant switching frequency, *IEEE Transactions on Industry Applications*, *35*(5), 1999, 1076–1082.

[7] T.G. Habetler, F. Profumo, M. Pastorelli, and L.M. Tolbert, Direct torque control of induction motor using space vector modulation, *IEEE Transactions on Industry Applications*, *28*, 1992, 1045–1053.

[8] X. Xu, R. DeDoncker, and D.W. Novotny, A stator flux oriented induction machine drive, *PESC 1988 Conf Rec.*, Kyoto, Japan, 870–876.

[9] X. Xue, X. Xu, T.G. Habetler, and D.M. Divan, A low cost stator flux oriented voltage source variable speed drive, *IEEE IAS Ann. Mtg. Conf Rec.*, 1990, 410–415.

[10] Y. Kumsuwana, S. Premrudeepreechacharna, and H.A. Toliyatb, Modified direct torque control method for induction motor drives based on amplitude and angle control of stator flux, *Electric Power Systems Research*, *78*(10), 2008, 1712–1718.

[11] K.-B. Lee, J.-H. Song, I. Choy, and J.-Y. Yoo, Improvement of low-speed operation performance of DTC for three-level inverter-fed induction motors, *IEEE Transactions on Industry Electronics*, *48*(5), 2001, 1006–1014.

[12] T. Noguchi, M. Yamamoto, S. Kondo, and I. Takahashi, Enlarging switching frequency in direct torque-controlled inverter by means of dithering, *IEEE Transactions on Industry Applications*, *35*(6), 1999, 1358–1366.

[13] N.R.N. Idri and A.H.M. Yatim, Direct torque control of induction machines with constant switching frequency and reduced torque ripple, *IEEE Transactions on Industrial Electronics*, *51*(4), 2004, 758–767.

[14] Y.-S. Lai, W.-K. Wang, and Y.-C. Chen, Novel switching techniques for reducing the speed ripple of AC drives with direct torque control, *IEEE Transactions on Industrial Electronics*, *51*(4), 2004, 768–775.

[15] G.S. Buja and M.P. Kazmierkowski, Direct torque control of PWM inverter-fed AC motors – A survey, *IEEE Transactions on Industrial Electronics*, *51*(4), 2004, 744–757.

[16] Ma.Á.M. Prats, G. Escobar, E. Galván, J.M. Carrasco, and R. Portillo, A switching control strategy based on output regulation subspaces for the control of induction motors using a three-level inverter, *IEEE Power Electronics Letters*, *1*(2), 2003, 29–32.

[17] A. Nabae, I. Takahashi, and H. Agaki, A new neutral point-clamped PWM inverter, *IEEE Transactions on Industrial Applications*, *17*, 1981, 518–523.

[18] S. Mukherjee and G. Poddar, Direct torque control of squirrel cage induction motor for optimum current ripple using three-level inverter, *IET Power Electronics*, *3*(6), 2010, 904–914.

[19] V.T. Somasekhar and K. Gopakumar, Three-level inverter configuration cascading two two-level inverters, *IEE Proceedings of Electric Power Applications*, *151*(2), 2003, 230–238.

[20] V. Kumar and S. Rao, Modified direct torque control of three phase induction motor drives with low ripple in flux and torque, *Leonardo Journal of Sciences (LJS)*, *18*, 2011, 27–44.

[21] J. Zhang and M.F. Rahman, Analysis and design of a novel direct flux control scheme for induction machine, *International Conference on IEMDC*, San Antonio, TX, 2005, 426–430.

[22] T.V. Kumar and S.S. Rao, Direct torque control method for induction motor drives based on modified amplitude and angle decoupled control of stator flux, *IEEE Conference PEDES-2010*, India, 2010.

Biographies

Vinay T. Kumar received his B. Tech. degree in electrical and electronics engineering from Jawaharlal Nehru Technological University (JNTU), Hyderabad, India in 2005 and his M. Tech. degree from JNTU, Hyderabad, India in 2008. He is presently doing research in the power electronics and drives area at the National Institute of Technology (NIT), Warangal, India.

Srinivasa S. Rao received his B. Tech. degree in electrical engineering from Regional Engineering College (REC), Warangal, India, in 1992 and M. Tech. degree from REC, Calicut, India, in 1994. He obtained his Ph.D. degree from NIT, Warangal in 2007. Since 1996, he has worked as a faculty member at NIT, Warangal, India. His research interests include power electronic drives, switch mode power converters, DSP controlled drives, and renewable energy generation. He is a life member of the System Society of India and the Indian Society of Technical Education. He is also a member of the Institution of Engineers (India).